Liquid Crystals

Publication details, including instructions for authors and subscription information:
http://www.informaworld.com/smpp/title~content=t713926090

Liquid crystalline properties of salicylaldimine-based dimers: influence of terminal alkyl chain length and central part

Remko Achten[a]; Arie Koudijs[a]; Zbigniew Karczmarzyk[b]; Antonius T. M. Marcelis Corresponding author[a]; Ernst J. R. Sudhölter[a]
[a] Laboratory of Organic Chemistry, Wageningen University, 6703 HB Wageningen, The Netherlands [b] Department of Chemistry, University of Podlasie, 08-110 Siedlce, Poland

To cite this Article Achten, Remko , Koudijs, Arie , Karczmarzyk, Zbigniew , Marcelis Corresponding author, Antonius T. M. and Sudhölter, Ernst J. R.(2004) 'Liquid crystalline properties of salicylaldimine-based dimers: influence of terminal alkyl chain length and central part', Liquid Crystals, 31: 2, 215 — 227

To link to this Article: DOI: 10.1080/02678290310001642531

URL: http://dx.doi.org/10.1080/02678290310001642531

Liquid Crystals, Vol. 31, No. 2, February 2004, 215–227

Liquid crystalline properties of salicylaldimine-based dimers: influence of terminal alkyl chain length and central part

REMKO ACHTEN, ARIE KOUDIJS, ZBIGNIEW KARCZMARZYK†,
ANTONIUS T. M. MARCELIS* and ERNST J. R. SUDHÖLTER
Laboratory of Organic Chemistry, Wageningen University, Dreijenplein 8,
6703 HB Wageningen, The Netherlands
†Department of Chemistry, University of Podlasie, ul. 3 Maja 54,
08-110 Siedlce, Poland

(*Received 14 May 2003; in final form 17 September 2003; accepted 26 September 2003*)

The synthesis and thermotropic properties of four homologous series of salicylaldimine-based dimer liquid crystals are reported. Two 4-(4-alkoxy-2-hydroxybenzylideneamino)benzoyloxy groups are connected to a central part consisting of a 1,3-phenylene, 1,5-pentylene, 2,2-dimethyl-1,5-pentylene or 3,3-dimethyl-1,5-pentylene unit. The terminal alkoxy chains have been varied from 4 to 16 carbon atoms in length. All the compounds exhibit liquid crystalline phases whose behaviour depends on the nature of the central part and the length of the alkoxy terminal chains. All compounds of the series with the central phenyl part exhibit enantiotropic B-phases, and the sequence B_6–B_1–B_2 on increasing terminal chain length was observed. Replacement of the phenyl group with a pentyl central group partly suppresses the formation of B-phases. The longer homologues of this series show the B_1 phase, while the shorter exhibit an intercalated SmC_c mesophase. The introduction of methyl substituents to the pentyl spacer causes the melting points to fall dramatically and the formation of B-phases is totally suppressed. The compounds with the long tails show intercalated SmA_c phases and those with short tails show intercalated SmC_c phases.

1. Introduction

Before 1996 (anti)ferroelectricity in liquid crystals was restricted to phases consisting of molecules with a chiral molecular structure. Niori *et al.* [1] were however the first to report this striking phenomenon in phases composed of non-chiral molecules with a bent or banana shape. In recent years a variety of banana-shaped molecules have been synthesized and studied. Banana-shaped compounds can form new smectic and two-dimensional ordered phases which are unlike those obtained from normal calamitic molecules. According to recommendations of the workshop on Banana-shaped Liquid Crystals: Chirality by Achiral Molecules, held in Berlin in 1997, these phases are simply designated B_1 to B_7. Since this nomenclature does not take the structure and symmetry of the mesophase into account it can be considered as a preliminary nomenclature. At this moment it is still difficult to establish a direct relationship between observed optical microscopy textures and phase assignment.

Of the seven B-phases known to date, the B_3 and B_4 phase [2] are 'solid-like'; the B_4 phase is also designated as the 'blue phase' [3]. The B_1 (Col_r) phase is a two-dimensional periodic phase [4, 5] and the B_6 phase can be compared to an intercalated SmC phase, but is generated by bent molecules [2].

Three of the phases possess electro-optical switching properties. The B_2 ($SmCP_A$) phase, first described by Niori *et al.* [1], is the most frequently investigated banana mesophase which is associated with antiferroelectric characteristics. The B_5 mesophase has an additional short range order within the layer, but shows the same electro-optic response as the B_2 phase [6]. The B_7 phase corresponds to different phases all exhibiting the characteristic textures seen in the original B_7 phase of nitro compounds [7]. The structure of the B_7 phase has not yet been elucidated and seems to be rather complex. 'New' banana phases have already been reported [8] and it is very likely that additional new mesophases will be reported in the future.

To understand the relationship between molecular structure and mesomorphic properties, banana-shaped compounds can be designed in numerous different ways. Most molecules that exhibit banana-phases (containing five, six or seven phenyl rings) are composed of symmetrical resorcinol derivatives substituted at the 1 and

---

*Author for correspondence; e-mail: ton.marcelis@wur.nl

Liquid Crystals ISSN 0267-8292 print/ISSN 1366-5855 online © 2004 Taylor & Francis Ltd
http://www.tandf.co.uk/journals
DOI: 10.1080/02678290310001642531

3 position [8–13]. Also the 3,4′-disubstituted biphenyl central fragment has proved to be a suitable building block for obtaining banana-shaped molecules [5, 14, 15]. Another way to design molecules with a bent shape is by the introduction of a central alkylene chain with an odd number of flexible units between two mesogenic units [16–19]. These compounds however are not so often studied as their aromatic counterparts. Compounds with an even number of flexible units between the two mesogenic groups have also been reported to show switching properties [20]. The introduction of substituents to the central spacer seems to promote the formation of intercalated layer structures [21, 22]. The linking groups between the wings of the aromatic fragments of the bent-shaped molecule can also be varied, and the most common are the imine and ester linking groups. The introduction of lateral substituents (fluorine [23], chlorine [24, 25], methyl [26], methoxy [27], cyano [28, 29], nitro [30], bromine [31] or a combination of different substituents [30, 32]) in the wings or in the central part of a banana-shaped compound is also used to modify the thermotropic properties of bent-shaped molecules. The length of the terminal alkyl(oxy) chain or fluorination of the terminal chain can also have a pronounced effect on the mesomorphic properties of compounds with bent-shaped molecules.

In recent years several homologous series of banana-shaped compounds have been synthesized and studied. In most cases a limited number of homologues were prepared; in particular, compounds with short terminal chains are often missing. In place of the unstable, light and moisture sensitive imine bond which is often used in banana-shaped compounds, we have prepared four series of more stable salicylaldimine-based dimers with terminal chains ranging from 4 to 16 carbon atoms in length. In order to study the influence of the central part of the molecule on the liquid crystalline properties we prepared the four series of compounds so that the nature of the connecting group between the two salicylaldimine wings was varied: phenyl (series **I-*n***), pentyl (series **II-*n***), 2,2-dimethylpentyl (series **III-*n***) and 3,3-dimethylpentyl (**IV-*n***) (figure 1). Three compounds of the **I-*n*** series (***n***=9, 10 and 16) have been extensively studied by other groups [33–35], and the **II-*n*** series was partly studied by Yelamaggad *et al.* [36]. In the present study we describe all compounds of the **I-*n*** and **II-*n*** series (n=4–12, 14 and 16). In addition we have prepared and studied two series in which the central pentyl spacer was symmetrically substituted (**IV-*n***) and non-symmetrically substituted (**III-*n***) with two methyl groups.

2. Experimental

2.1. *Synthesis*

The four series of compounds were prepared according to the scheme. For the series with the

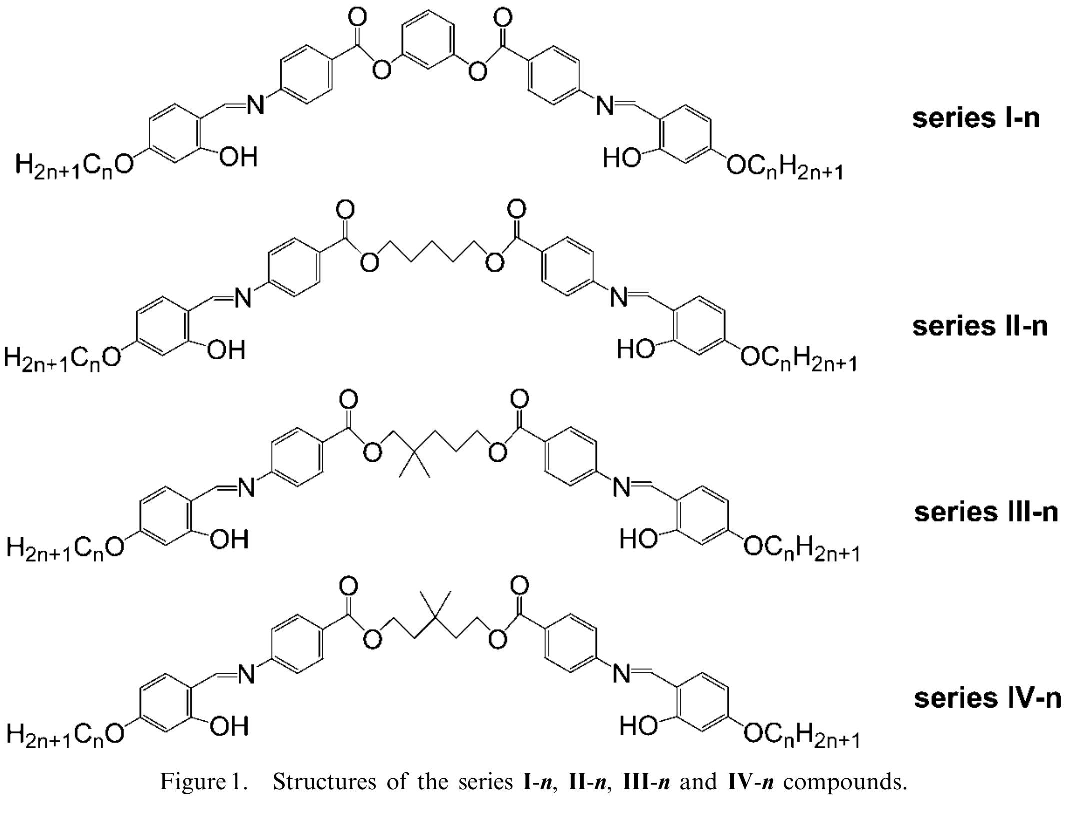

Figure 1. Structures of the series **I-*n***, **II-*n***, **III-*n*** and **IV-*n*** compounds.

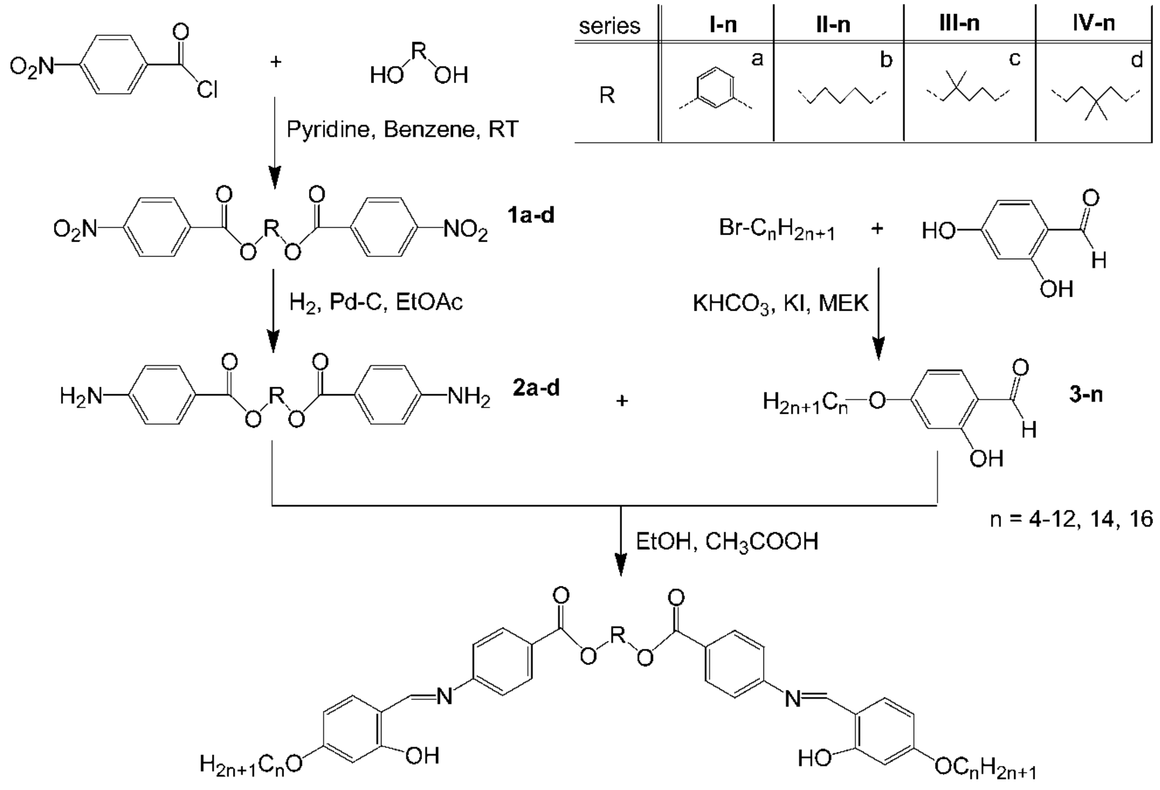

Scheme. Synthetic pathways for the series **I-*n***, **II-*n***, **III-*n*** and **IV-*n*** compounds.

methyl-substituted pentyl spacers (series **III-*n*** and **IV-*n***) the diols were prepared by reduction of the appropriate substituted glutaric acids with $LiAlH_4$ in THF, according to the method used by Eilbracht *et al.* [37]. For the **I-*n*** and **II-*n*** series the central diols (resorcinol and 1,5-pentanediol) were obtained from Aldrich. The synthesis of the aldehydes **3-*n*** was performed according to literature procedures [36].

The bis(4-nitrobenzoate) compounds **1a–d** were prepared by treating 4-nitrobenzoyl chloride with the appropriate diol in the presence of pyridine. Subsequently, the dinitro compounds **1a–d** were reduced by catalytic hydrogenation (H_2/Pd-C) to yield the diamines **2a–d**. The alkoxybenzaldehydes **3-*n*** were prepared by heating 2,4-dihydroxybenzaldehyde with 1-*n*-bromoalkanes in the presence of $KHCO_3$ and a catalytic amount of KI in MEK. Finally, the desired compounds were obtained by condensing 2-hydroxy-4-*n*-alkoxybenzaldehyde **3-*n*** with the diamino compounds **2a–d**.

All dimers gave NMR spectra in agreement with the proposed structure, and showed correct elemental analysis.

Since the preparation of the bis(4-nitrobenzoate) compounds **1a** and **1b** and the diamines **2a** and **2b** have been described elsewhere [34, 36], we will only describe the synthesis of compounds **1c**, **1d**, **2c** and **2d**. From the final list of liquid crystal compounds we will describe the synthesis of one short-tailed ($n=7$) and one long-tailed ($n=14$) compound of each series.

2.1.1. *1,5-Bis(4-nitrobenzoyloxy)-2,2-dimethylpentane, 1c*

In a 250 ml round-bottomed flask equipped with a nitrogen inlet and a septum, 1.32 g (10.0 mmol, 1 equiv.) of 2,2-dimethyl-1,5-pentanediol was dissolved in 20 ml of dry pyridine and 20 ml of dry benzene. The solution was then cooled in an ice-bath and a solution of 4-nitrobenzoyl chloride (4.65 g, 25 mmol, 2.5 equiv.) in 20 ml of dry benzene was added dropwise. The reaction mixture was stirred for 24 h at room temperature; it was then acidified with 3M HCl and extracted twice with CH_2Cl_2. The combined organic layers were washed successively with 1M NaOH (twice) and brine. The organic layer was dried over Na_2SO_4 and filtered; the filtrate was concentrated and the residue recrystallized from $CHCl_3$/MeOH. Yield 84%, m.p. 114°C. ^1H NMR (200 MHz, $CDCl_3$): δ 8.30–8.15 (m, 8H, Ar), 4.37 (t, 2H, OCH_2), 4.13 (s, 2H, OCH_2C), 1.80 (m, 2H, CH_2), 1.54 (m, 2H, CCH_2), 1.07 (s, 6H, 2 × CH_3). Elemental analysis for $C_{21}H_{22}N_2O_8$ ($M=430.41$): calc. C 58.60, H 5.15, N 6.51; found C 58.21, H 5.07, N 6.36%.

2.1.2. *1,5-Bis(4-nitrobenzoyloxy)-3,3-dimethylpentane,* ***1d***

This compound was prepared similarly to **1c**, from 3,3-dimethyl-1,5-pentanediol and 4-nitrobenzoyl chloride. Yield 91%, m.p. 98–99°C. ^{1}H NMR (200 MHz, $CDCl_3$): δ 8.27 (d, 4H, Ar), 8.17 (d, 4H, Ar), 4.48 (t, 4H, $2\times OCH_2$), 1.84 (t, 4H, $2\times CH_2$), 1.10 (s, 6H, $2\times CH_3$). Elemental analysis for $C_{21}H_{22}N_2O_8$ (M=430.41): calc. C 58.60, H 5.15, N 6.51; found C 58.27, H 4.96, N 6.45%.

2.1.3. *1,5-Bis(4-aminobenzoyloxy)-2,2-dimethylpentane,* ***2c***

A mixture of 3.60 g (8.4 mmol) of compound **1c**, 70 ml dry ethyl acetate and 200 mg Pd-C (10%) was hydrogenated in a Parr apparatus at 4 bar for 3 h. The reaction mixture was then filtered to remove the catalyst and the solvent evaporated, yielding the pure product in quantitative yield as an oil. ^{1}H NMR (200 MHz, $CDCl_3$): δ 7.82 (m, 4H, Ar), 6.61 (m, 4H, Ar), 4.24 (t, 2H, OCH_2), 4.00 (s, 2H, OCH_2C), 1.72 (m, 2H, CH_2), 1.52 (m, 2H, CCH_2), 1.01 (s, 6H, $2\times CH_3$).

2.1.4. *1,5-Bis(4-aminobenzoyloxy)-3,3-dimethylpentane,* ***2d***

This compound was prepared similarly to **2c**, from compound **1d**, in quantitative yield, m.p. 105–106°C. ^{1}H NMR (200 MHz, $CDCl_3$): δ 7.81 (d, 4H, Ar), 6.59 (d, 4H, Ar), 4.35 (t, 4H, OCH_2), 1.76 (t, 4H, CH_2), 1.04 (s, 6H, $2\times CH_3$). Elemental analysis for $C_{21}H_{26}N_2O_4$ (M=370.44): calc. C 68.09, H 7.07, N 7.56; found C 67.70, H 7.08, N 7.15%.

2.1.5. *General procedure for preparing the liquid crystals* ***I-n****,* ***II-n****,* ***III-n*** *and* ***IV-n***

A mixture of the bis(4-aminobenzoate) **2a**–**d** (0.5 mmol, 1 equiv.), 2-hydroxy-4-alkoxybenzaldehyde **3-*n*** (1.0 mmol, 2.0 equiv.), absolute ethanol (15 ml) and a few drops of acetic acid was heated under reflux for 2 h. After cooling, the yellow precipitate was collected by filtration and washed with hot absolute ethanol. The yellow crystals were finally recrystallized from methanol/chloroform; yield 50–75%.

1,3-Bis-[4-(2-hydroxy-4-heptyloxybenzylideneamino)-benzoyloxy]benzene, ***I-7***. ^{1}H NMR (200 MHz, $CDCl_3$): δ 13.38 (s, 2H, $2\times$–OH), 8.57 (s, 2H, $2\times$CH–N), 8.24 (d, 4H, Ar), 7.49 (t, 1H, Ar), 7.36–7.16 (m, 9H, Ar), 6.51 (m, 4H, Ar), 4.01 (t, 4H, $2\times OCH_2$), 1.80–1.32 (m, 20H, $10\times CH_2$), 0.89 (t, 6H, $2\times CH_3$). Elemental analysis for $C_{48}H_{52}N_2O_8$ (M=784.94): calc. C 73.45, H 6.68, N 3.57; found C 73.28, H 6.66, N 3.50%.

1,3-Bis-[4-(2-hydroxy-4-tetradecyloxybenzylideneamino)-benzoyloxy]benzene, ***I-14***. ^{1}H NMR (200 MHz, $CDCl_3$): δ 13.38 (s, 2H, $2\times$–OH), 8.57 (s, 2H, $2\times$CH–N), 8.24 (d, 4H, Ar), 7.50 (t, 1H, Ar), 7.37–7.21 (m, 9H, Ar), 6.51 (m, 4H, Ar), 4.01 (t, 4H, $2\times OCH_2$), 1.82–1.26 (m, 48H, $24\times CH_2$), 0.88 (t, 6H, $2\times CH_3$). Elemental analysis for $C_{62}H_{80}N_2O_8$ (M=981.31): calc. C 75.89, H 8.22, N 2.86; found C 75.71, H 8.23, N 2.82%.

1,5-Bis-[4-(2-hydroxy-4-heptyloxybenzylideneamino)-benzoyloxy]pentane, ***II-7***. ^{1}H NMR (200 MHz, $CDCl_3$): δ 13.42 (s, 2H, $2\times$–OH), 8.51 (s, 2H, $2\times$CH–N), 8.06 (d, 4H, Ar), 7.25 (m, 6H, Ar), 6.48 (m, 4H, Ar), 4.37 (t, 4H, $OCOCH_2$), 3.99 (t, 4H, $2\times OCH_2$), 1.92–1.31 (m, 26H, $13\times CH_2$), 0,90 (t, 6H, $2\times CH_3$). Elemental analysis for $C_{47}H_{58}N_2O_8$ (M=778.97): calc. C 72.47, H 7.50, N 3.60; found C 72.55, H 7.57, N 3.58%.

1,5-Bis-[4-(2-hydroxy-4-tetradecyloxybenzylideneamino)-benzoyloxy]pentane, ***II-14***. ^{1}H NMR (200 MHz, $CDCl_3$): δ 13.41 (s, 2H, $2\times$–OH), 8.51 (s, 2H, $2\times$CH–N), 8.06 (d, 4H, Ar), 7.25 (m, 6H, Ar), 6.47 (m, 4H, Ar), 4.37 (t, 4H, $OCOCH_2$), 3.99 (t, 4H, $2\times OCH_2$), 1.91–1.26 (m, 54H, $27\times CH_2$), 0,87 (t, 6H, $2\times CH_3$). Elemental analysis for $C_{61}H_{86}N_2O_8$ (M=975.34): calc. C 75.12, H 8.89, N 2.87; found C 74.84, H 8.86, N 2.81%.

1,5-Bis-[4-(2-hydroxy-4-heptyloxybenzylideneamino)-benzoyloxy]-2,2-dimethylpentane, ***III-7***. ^{1}H NMR (200 MHz, $CDCl_3$): δ 13.41 (s, 2H, $2\times$–OH), 8.50 (s, 2H, $2\times$CH–N), 8.04 (m, 4H, Ar), 7.21 (m, 6H, Ar), 6.45 (m, 4H, Ar), 4.33 (t, 2H, $OCOCH_2$), 4.09 (s, 2H, $OCOCH_2$), 3.98 (t, 4H, $2\times OCH_2$), 1.86–1.30 (m, 24H, $12\times CH_2$), 1.06 (s, 6H, CH_3CCH_3), 0,89 (t, 6H, $2\times CH_3$). Elemental analysis for $C_{49}H_{62}N_2O_8$ (M=807.03): calc. C 72.93, H 7.74, N 3.47; found C 72.93, H 7.79, N 3.42%.

1,5-Bis-[4-(2-hydroxy-4-tetradecyloxybenzylideneamino)-benzoyloxy]-2,2-dimethylpentane, ***III-14***. ^{1}H NMR (200 MHz, $CDCl_3$): δ 13.42 (s, 2H, $2\times$–OH), 8.50 (s, 2H, $2\times$CH–N), 8.05 (m, 4H, Ar), 7.22 (m, 6H, Ar), 6.45 (m, 4H, Ar), 4.33 (t, 2H, $OCOCH_2$), 4.09 (s, 2H, $OCOCH_2$), 3.98 (t, 4H, $2\times OCH_2$), 1.86–1.26 (m, 52H, $26\times CH_2$), 1.06 (s, 6H, CH_3CCH_3), 0,87 (t, 6H, $2\times CH_3$). Elemental analysis for $C_{63}H_{90}N_2O_8$ (M=1003.40): calc. C 75.41, H 9.04, N 2.79; found C 75.46, H 9.14, N 2.73%.

1,5-Bis-[4-(2-hydroxy-4-heptyloxybenzylideneamino)-benzoyloxy]-3,3-dimethylpentane, ***IV-7***. ^{1}H NMR (200 MHz, $CDCl_3$): δ 13.41 (s, 2H, $2\times$–OH), 8.45 (s, 2H, $2\times$CH–N), 8.03 (d, 4H, Ar), 7.22 (m, 6H, Ar), 6.46 (m, 4H, Ar), 4.44 (t, 4H, $OCOCH_2$), 3.98 (t, 4H, $2\times OCH_2$), 1.87–1.31 (m, 24H, $12\times CH_2$), 1.10 (s, 6H, CH_3CCH_3), 0,90 (t, 6H, $2\times CH_3$). Elemental analysis for $C_{49}H_{62}N_2O_8$ (M=807.03): calc. C 72.93, H 7.74, N 3.47; found C 72.53, H 7.65, N 3.41%.

1,5-Bis-[4-(2-hydroxy-4-tetradecyloxybenzylideneamino)-benzoyloxy]-3,3-dimethylpentane, ***IV-14***. ^{1}H NMR (200 MHz, $CDCl_3$): δ 13.41 (s, 2H, $2\times$–OH), 8.45 (s, 2H, 2 × CH–N), 8.03 (d, 4H, Ar), 7.22 (m, 6H, Ar), 6.45 (m, 4H, Ar), 4.44 (t, 4H, $OCOCH_2$), 3.97 (t, 4H, 2 × OCH_2), 1.89–1.26 (m, 52H, 26 × CH_2), 1.10 (s, 6H, CH_3CCH_3), 0,87 (t, 6H, 2 × CH_3). Elemental analysis for $C_{63}H_{90}N_2O_8$ (M = 1003.40): calc. C 75.41, H 9.04, N 2.79; found C 75.23, H 9.12, N 2.74%.

2.2. *Characterization*

Melting points, thermal phase transition temperatures and optical studies of the liquid crystalline phases were determined on samples between ordinary glass slides using an Olympus BH-2 polarized light microscope equipped with a Mettler FP82HT hot stage, which was controlled by a Mettler FP80HT central processor. Differential scanning calorimetry (DSC) thermograms were obtained on a Perkin Elmer DSC-7 system using 2–5 mg samples in 30 μL sample pans and a scan rate of 5°C min^{-1}. ΔH is expressed in J mol^{-1}. Temperature-dependent X-ray diffraction patterns were measured on a Philips X'pert Pro MRD instrument equipped with an Anton Paar camera for temperature control. For the measurements in the small angle region the sample was spread in the isotropic or liquid crystalline phase on a thin glass slide (about 15 μm thick) which was placed on a temperature-regulated flat copper sample stage. This sample preparation sometimes caused very high intensities of X-ray reflections (> 500 kc s^{-1}) because of partial or complete orientation of the molecules in the liquid crystalline state. For measurements in the wide angle region glass capillaries (diameter 0.5 mm, glass thickness 0.01 mm) were used.

3. Results and discussion

3.1. *The **I-n** series*

The thermotropic properties of the **I-*n*** series containing a central phenyl group are given in table 1, and the melting and isotropization temperatures are shown in figure 2. All the compounds in this series exhibit one enantiotropic liquid crystalline B-phase, its type depending on the length *n* of the terminal alkyl tail. Compound **I-16** has been described previously, and like Shankar Rao *et al.* [35] we observed the growth of thread-like and spiral nuclei upon cooling from the isotropic liquid. Characteristic optical textures are shown in figure 3 (*a*). The X-ray pattern we observed was also similar (figure 4). Based on these observations this phase was assigned as B_7. However, because the growth of spirals is not unique for the B_7 phase [38, 39], and because the X-ray pattern does not resemble the pattern of the original B_7 compound [7], we have serious doubts about this assignment. The X-ray pattern of **I-16**, which is similar to the patterns of **I-14** and **I-12**, indicates a lamellar structure with a *d*-spacing of 49.2 Å and weak higher order reflections. Since this layer spacing fits perfectly in the trend observed for compounds **I-7** to **I-14**, and because antiferroelectric switching behaviour was observed for **I-16** we assign this phase as B_2.

Table 1. Transition temperatures (°C), transition enthalpies (kJ mol^{-1}; in square brackets) and layer spacings *d* (Å) of the **I-*n*** series.

n	Cr	B_6	B_1	B_2	I	*d*
4	● 188 [36]	● 196 [13]			●	17.8
5	● 160 [32]		● 179 [16]		●	37.2
6	● 143 [11]		● 174 [17]		●	38.6
7	● 128 [20]			● 173.5 [17]	●	36.4
8	● 126 [20]			● 174.5 [18]	●	37.9
9	● 119 [19]			● 176.5 [19]	●	39.7
10	● 117 [20]			● 178.5 [21]	●	41.1
11	● 114 [20]			● 177 [20]	●	42.2
12	● 114 [21]			● 178 [22]	●	43.8
14	● 112 [21]			● 175 [23]	●	46.6
16	● 113 [76]			● 172 [23]	●	49.2

Compounds **I-9** and **I-10** have been described previously in the literature [33, 34]. As for several other series the longer homologues of the **I-*n*** series exhibit the B_2 mesophase. An example of the textures observed for these compounds is given in figure 3 (*b*) for compound **I-12**; it shows similarities with those found for other B_2 phases [2]. Upon cooling from the isotropic liquid a smectic focal-conic texture develops. X-ray diffraction patterns of the compounds that exhibit the liquid crystalline B_2 phase (**I-7** to **I-14**) all show a significant similarity to those observed for B_2 phases consisting of other bent-shaped molecules [10] (figure 4). Together with the optical texture, the X-ray patterns of oriented samples indicate a tilted smectic in

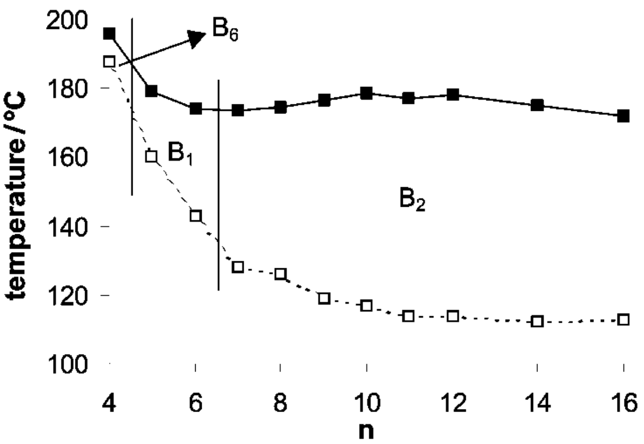

Figure 2. Dependence of the melting points (---□---) and isotropization temperatures (—■—) of series **I-*n*** on the number of carbon atoms *n* in the terminal chains.

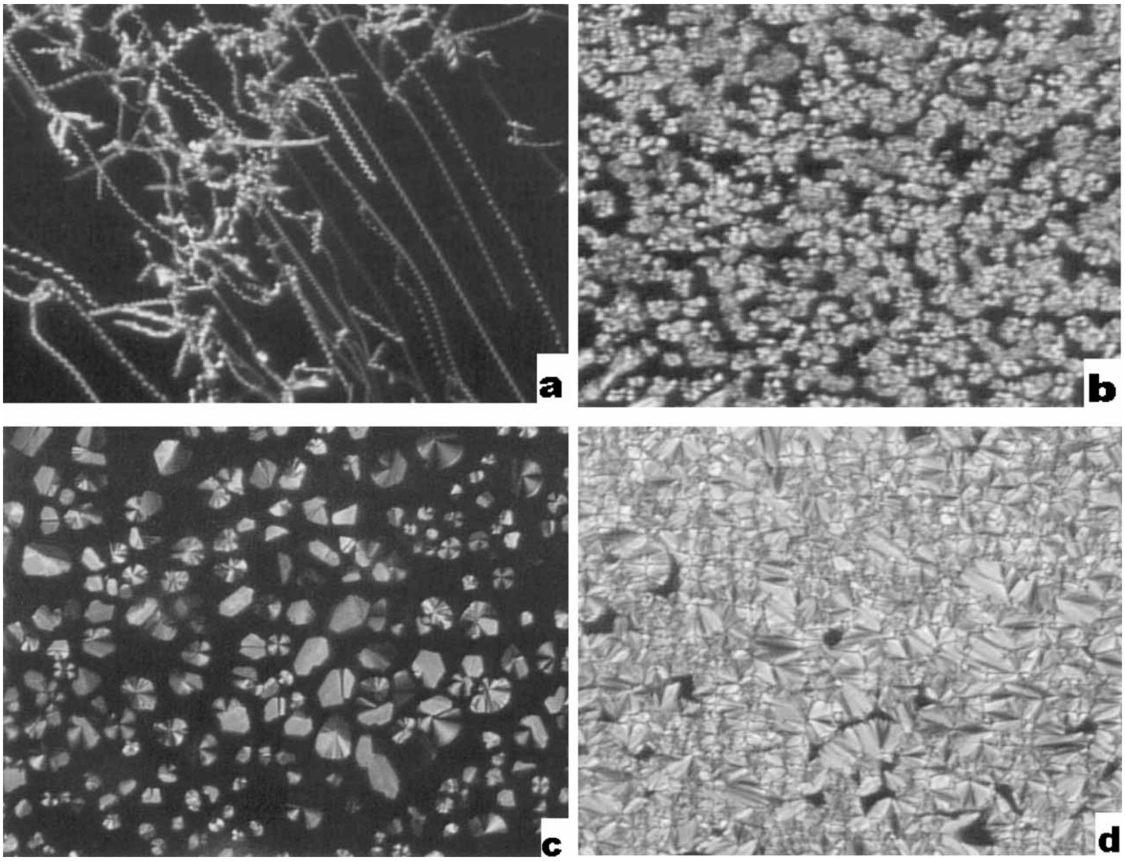

Figure 3. Photomicrographs of the textures observed on cooling from the isotropic state for series **I-*n***. (*a*) **I-16**, B_2; (*b*) **I-12**, B_2; (*c*) **I-6**, B_1; (*d*) **I-4**, B_6.

which the layer spacings increase linearly from 36.4 Å for **I-7** to 46.6 Å for **I-14** (table 1). A broad peak in the wide angle region proves the liquid-like order within the layers (not shown).

For the short-tailed members (**I-5** and **I-6**) of the **I-*n*** series, the B_1 phase was observed on cooling from the isotropic state by the formation of small bâtonnets which coalesce into a mosaic-like texture, figure 3 (***c***). For the B_1 phase a rectangular columnar structure was proposed by Watanabe *et al.* [4]. The X-ray diffractogram of compound **I-6** (figure 4) exhibits two reflections in the small angle region, pointing to a two-dimensional rectangular cell. These two reflections in the small angle region of the B_1 phase have been evaluated on the basis of a rectangular cell by analogy to the B_1 phase of other compounds [10, 28]. The periodicities d_1 and d_2 for **I-6** in the small angle region are 28.8 and 19.3 Å, respectively. The corresponding lattice parameters for a modulated phase with a rectangular lattice, assuming the reflection indexing (0 0 2) and (1 0 1), are $a = 43.3$ Å for the in-plane parameter and $c = 38.6$ Å for the layer thickness (table 1). Assuming a molecular length of 44.4 Å the calculated molecular tilt is 30°. For **I-5** the periodicities d_1 and d_2 in the small angle region are 25.0 and 18.6 Å, respectively. The corresponding lattice parameters are $a = 33.7$ Å and $c = 37.2$ Å. Assuming a molecular length of 41.9 Å the calculated molecular tilt is 27°. Tilt angles of 25–30° for the B_1 phase have been reported previously in the literature [10, 12].

Compound **I-4** shows only one reflection in the small angle region (figure 4). The corresponding period is smaller than half the molecular length. In consideration with the fan-shaped optical texture, figure 3 (*d*), this mesophase was assigned as the intercalated B_6 phase.

In conclusion, the **I-*n*** series shows the phase sequence B_6–B_1–B_2 with increasing terminal chain length. This sequence has been reported previously [12, 40]; in these series, however, there were always one or more compounds exhibiting two mesophases.

3.2. *The **II-n** series*

Six compounds ($n = 6$, 8, 10, 11, 12 and 16) of the **II-*n*** series with the pentyl spacer have been described by Yelamaggad *et al.* [36]. We have synthesized additional intermediate and short-tailed homologues. The

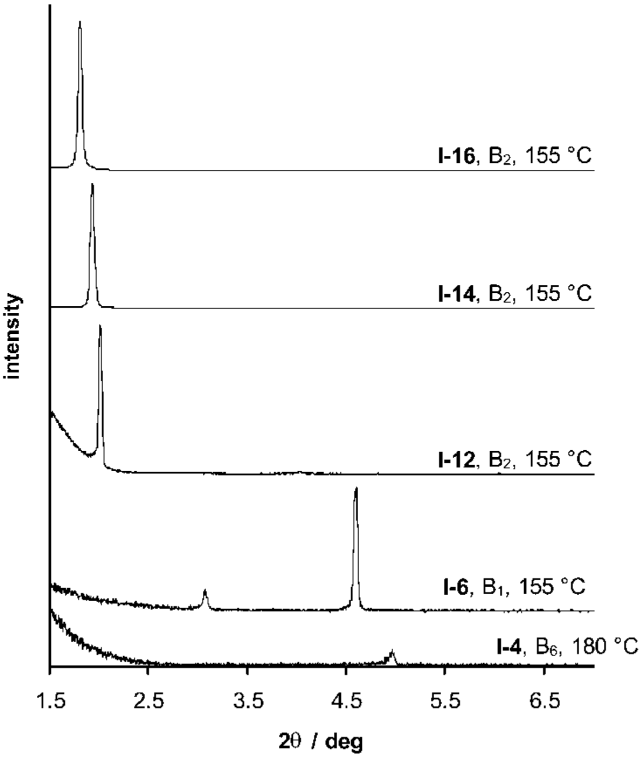

Figure 4. X-ray intensity profiles of oriented samples of series **I-*n***.

thermotropic properties of series **II-*n*** are given in table 2 and are very similar to the reported values. The melting points and isotropization temperatures are shown in figure 5. All the compounds in the **II-*n*** series show liquid crystalline properties.

Only the long- and short-tailed compounds exhibit enantiotropic mesophases. The longer ($n = 14$ and 16) homologues show the two-dimensional B_1 phase. On cooling from the isotropic phase the B_1 phase appears as a mosaic texture with spherulitic domains, figure 6 (*a*).

Table 2. Transition temperatures (°C), transition enthalpies (kJ mol^{-1}; in square brackets) and layer spacings d (Å) of the **II-*n*** series.

n	Cr	SmC_c	B_1	I	d
4	● 134 [33]	● 160 [12]		●	19.4
5	● 142 [41]	● 151 [12]		●	20.2
6	● 142 [41]	● 147 [13]		●	21.0
7	● 143 [57]	(● 141 [13])		●	21.8
8	● 141 [56]		(● 139 [a])	●	a
9	● 140 [57]		(● 138 [14])	●	a
10	● 139 [59]		(● 137 [16])	●	a
11	● 138 [61]		(● 136 [a])	●	a
12	● 138 [42]		● 138 [17]	●	a
14	● 133 [42]		● 136 [17]	●	51.3
16	● 131 [41]		● 135 [16]	●	53.9

[a] Could not be determined.

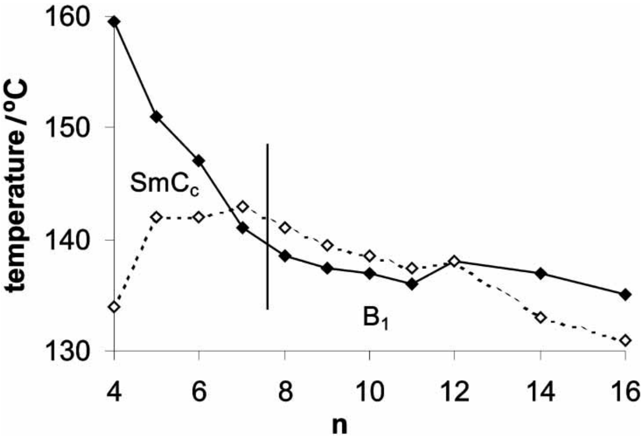

Figure 5. Dependence of the melting points (---◇---) and isotropization temperatures (—◆—) of series **II-*n*** on the number of carbon atoms n in the terminal chains.

X-ray measurements for **II-14** and **II-16** show patterns similar to those described in the literature [36]. The compounds with intermediate length tails ($n = 8$–11) show a similar B_1 mesophase according to polarized light microscopy observations figure 6 (*c*). It was impossible however to make X-ray measurements on these monotropic compounds since crystallization occurred very soon after formation of the liquid crystalline mesophase. Compound **II-12** showed a different optical texture. Specifically, the growth of spiral and double-spiral germs within the isotropic melt was observed.

The liquid crystalline phases of the shorter homologues of the **II-*n*** series ($n = 4$–7) were identified as intercalated SmC mesophases (SmC_c). Upon cooling from the isotropic phase a focal-conic texture appeared, figure 6 (*d*). Simultaneously, the Schlieren optical texture was also observed. The sharp first order reflection in the low angle region of the XRD pattern points to a layer spacing less than half the length of the molecule in the most extended conformation (table 2). In the wide angle region a broad peak is present, characteristic of a liquid-like arrangement of the molecules within the layers. Based on these observations we conclude that this phase is the intercalated SmC_c mesophase.

3.3. *The III-n series*

Table 3 lists the thermotropic properties of the non-symmetric **III-*n*** series. The dependence of the transition temperatures on the length of the terminal alkyl chains is shown in figure 7. Compared with the **II-*n*** series the liquid crystalline range is larger, mainly as a result of the lower melting points. On cooling from the isotropic phase the longer members ($n = 9$–16) of the **III-*n*** series form focal conic fans, which implies a smectic layered structure. Upon shearing the glass slides dark areas

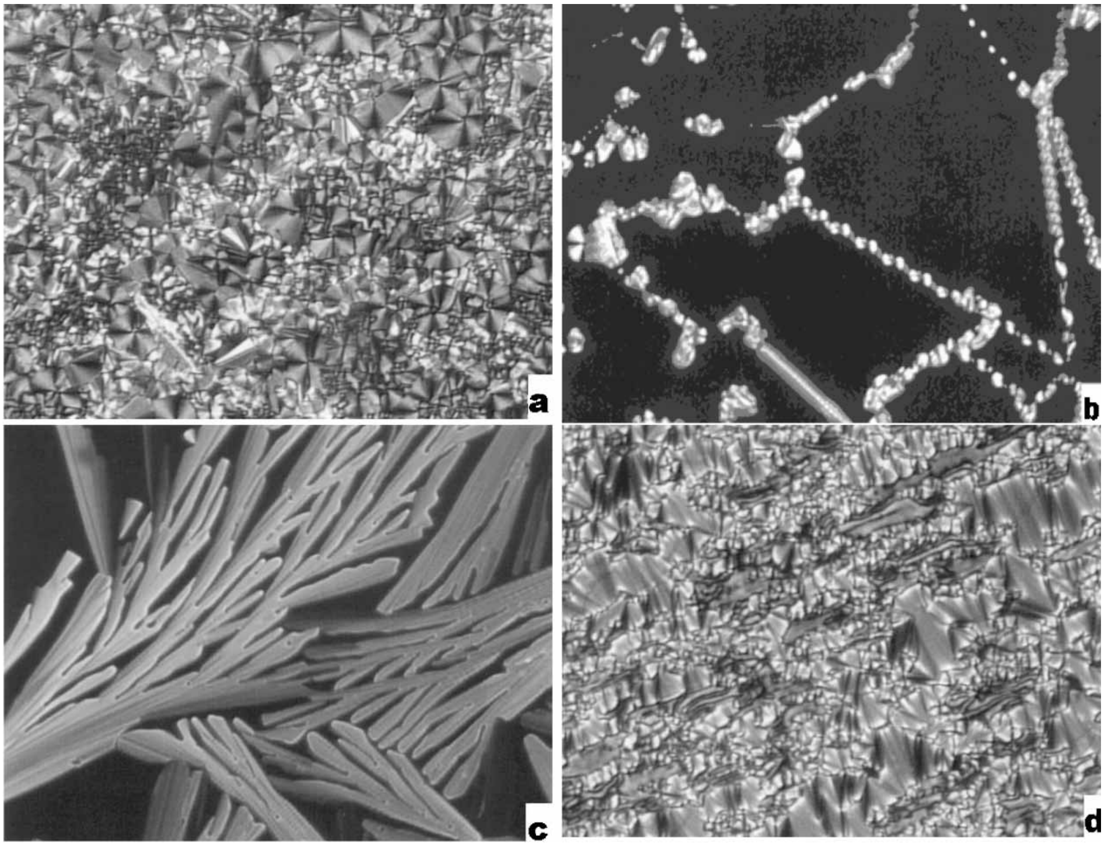

Figure 6. Photomicrographs of the textures observed on cooling from the isotropic state for series **II-*n***. (*a*) **II-16**, B_1; (*b*) **II-12**, B_1 or B_7; (*c*) **II-8**, B_1; (*d*) **II-6**, SmC_c.

were observed containing no Schlieren textures, indicating an orthogonal arrangement of the director with respect to the layer planes. XRD patterns show broad peaks in the wide angle region. In the small angle region, the first order Bragg peak is observed corresponding to the (0 0 1) planes. For the compounds **III-9** to **III-16** the layer spacings are approximately half the estimated molecular lengths, resulting in a *d*/*l* ratio of ~0.5 (table 3). Consequently, this mesophase is assigned as an intercalated SmA phase (SmA_c).

For the compounds of the **III-*n*** series with short tails ($n = 4$–8), spherulitic domains and focal-conics are seen,

Table 3. Transition temperatures (°C), transition enthalpies (kJ mol^{-1}; in square brackets) and layer spacings *d* (Å) of the **III-*n*** series.

n	Cr	SmC_c	SmA_c	I	*d*
4	• 97.5 [27]	• 139.5 [10]		•	20.8
5	• 99 [23]	• 135 [12]		•	21.8
6	• 97 [24]	• 135 [12]		•	22.6
7	• 95 [37]	• 133 [12]		•	23.9
8	• 97.5 [38]	• 132 [12]		•	25.2
9	• 97 [39]		• 132 [12]	•	27.8
10	• 102 [47]		• 133 [12]	•	29.6
11	• 96 [37]		• 133 [12]	•	30.9
12	• 101 [44]		• 134 [13]	•	32.3
14	• 109 [56]		• 135 [13]	•	34.8
16	• 112 [78]		• 135 [14]	•	37.5

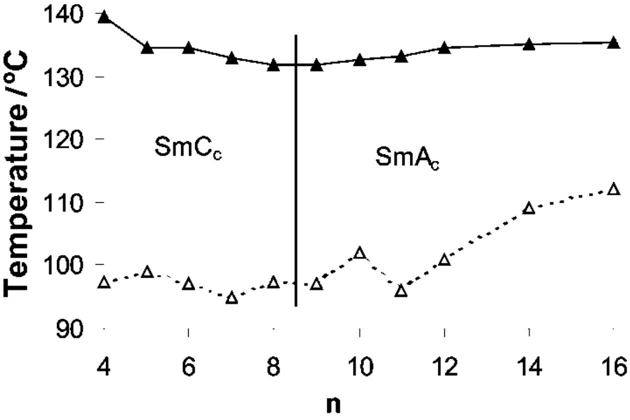

Figure 7. Dependence of the melting points (---△---) and isotropization temperatures (—▲—) of series **III-*n*** on the number of carbon atoms ***n*** in the terminal chains.

figure 8 (*a*). On cooling from the isotropic melt, fan-shaped textures were also observed in a dendritic-like texture, figure 8 (*b*). Schlieren textures were observed in the homeotropic regions of the sample indicating a tilted phase. X-ray measurements show broad peaks in the wide angle region, and given the small *d*-spacings, this mesophase is assigned as an intercalated $\mathrm{SmC_c}$ phase. Table 3 lists the layer spacings of the phases seen for the **III-*n*** compounds.

In the **III-*n*** series the intercalated $\mathrm{SmC_c}$ phase is present for the short homologues, as seen also for the non-substituted **II-*n*** series. The longer homologues of the **II-*n*** series show the $\mathrm{B_1}$ phase which is replaced by the intercalated $\mathrm{SmA_c}$ phase in the substituted **III-*n*** series. Substitution of the central spacer seems to suppress formation of the $\mathrm{B_1}$ mesophase because of steric reasons. The densely packed core of columns in the $\mathrm{B_1}$ phase can not form because of the dimethyl substituents. Replacement of the $\mathrm{B_1}$ phase with the intercalated $\mathrm{SmA_c}$ phase is unexpected, however, since the terminal alkyl chains are much longer than half the spacer length. In general the formation of intercalated layer structures in dimeric compounds is promoted if the terminal chain lengths are shorter than half the spacer length. A smectic monolayer is in general observed if the terminal chains are longer than half the length of the spacer [41]. In the latter case a microphase separation occurs into three regions: mesogenic groups, spacers and terminal chains. On the other hand, the presence of substituents on the central spacer has been shown to promote formation of intercalated smectic phases [21, 22].

The presence of an intercalated layer structure has previously been explained in terms of either an increase in entropy gained from the homogeneous mixing of the mesogenic moieties, an electrostatic quadrupolar interaction, or by an excluded volume or space-filling constraint [42]. From the study performed by Blatch and Luckhurst [43], it was suggested that some specific (dipolar) interaction is required between different mesogenic groups to stabilize the intercalated structure.

A transition from the intercalated $\mathrm{SmA_c}$ to the intercalated $\mathrm{SmC_c}$ phase upon decreasing the terminal chain length such as seen for the **III-*n*** series, has to our knowledge only once been reported in the literature [44]. In a series studied by Weissflog *et al.*, three-ring mesogenic units connected via a bis(carbonyloxy)propylene spacer exhibited thermotropic properties comparable to the **III-*n*** series. The most important difference in properties between the two series is the absence of intermediate compounds in the **III-*n*** series that possess both smectic modifications in one compound. In particular, the occurrence of the intercalated $\mathrm{SmA_c}$ mesophase despite the odd-numbered spacer (which favours, in general, a bent molecular structure [42, 45]) is an unexpected phenomenon. Two possible reasons were suggested for this phenomenon [44]. First, the stabilization of the $\mathrm{SmA_c}$ phase on increasing the chain length could be related to a stretching of the spacer, favoured because of space filling conditions. Second, the strong lateral cohesion of the mesogenic moieties could be enhanced by the antiparallel aligned dipoles of the mesogenic units.

3.4. *The IV-n series*

In the **IV-*n*** series the pentyl spacer is substituted with two methyl groups at the central carbon atom. The thermotropic properties and layer spacings *d* of this series are given in table 4 and the melting points and isotropization temperatures shown in figure 9.

The compounds of this series show wider liquid crystalline ranges than those of series **II-*n***, and mainly as a result of lower melting points. The thermotropic

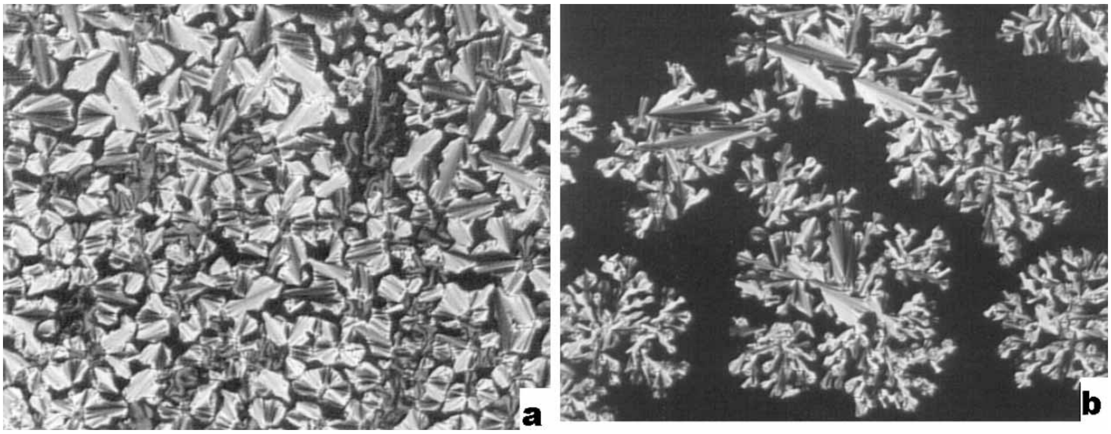

Figure 8. Photomicrographs of the textures observed on cooling from the isotropic state for series **III-*n***. (*a*) **III-7**, $\mathrm{SmC_c}$; (*b*) **III-5**, $\mathrm{SmC_c}$.

Table 4. Transition temperatures (°C), transition enthalpies (kJ mol^{-1}; in square brackets) and layer spacings *d* (Å) of the **IV-*n*** series.

n	Cr	SmA$_c$	SmC$_c$	SmA$_c$	I	*d*
4	● 102 [43]	● 121 [0.7]	● 157 [11]		●	22.8/21.5
5	● 118 [36]		● 153 [12]		●	22.9
6	● 112 [33]		● 151 [12]		●	24.0
7	● 113 [39]		● 149 [13]		●	25.3
8	● 109 [40]			● 148 [13]	●	27.1
9	● 102 [56]			● 147 [13]	●	28.8
10	● 100 [59]			● 147 [14]	●	30.1
11	● 99 [55]			● 148 [15]	●	31.4
12	● 99 [65]			● 149 [15]	●	32.7
14	● 101 [105]			● 149 [15]	●	35.3
16	● 104 [125]			● 148 [17]	●	37.9

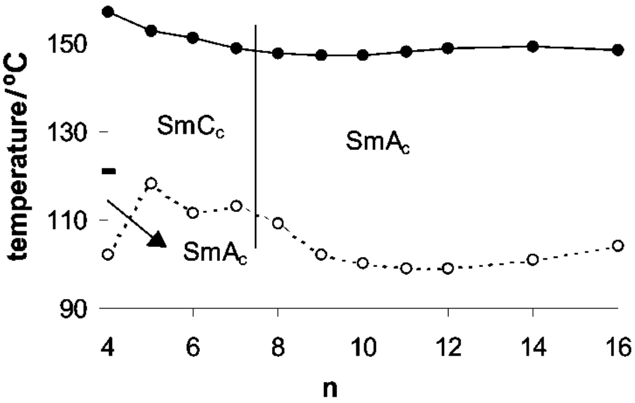

Figure 9. Dependence of the melting points (---○---) and isotropization temperatures (—●—) of series **IV-*n*** on the number of carbon atoms *n* in the terminal chains. The vertical line denotes the SmA$_c$ to SmC$_c$ transition.

behaviour of this series is very similar to that of the **III-*n*** series. As in the non-symmetrical **III-*n*** series, the compounds with long alkyl tails exhibit the intercalated SmA$_c$ phase. For the short homologues the intercalated SmC$_c$ phase is observed.

Compound **IV-4** exhibits an additional low temperature phase which is absent in the **III-*n*** series. Upon cooling the SmC$_c$ phase of **IV-4** a texture appears in which homeotropic regions with no birefringence are observed. These optical textures are typical of a SmA phase. The XRD pattern for the **IV-4** compound shows no changes in the wide angle region at this transition, so a more highly ordered mesophase, such as the SmB phase can be excluded. The layer thickness increases slightly from 21.5 to 22.8 Å at the transition; this corresponds to half the molecular length. Therefore, we conclude that this low temperature mesophase is probably a SmA$_c$ phase.

The inverse phase sequence SmA→SmC with increasing temperature is unusual but not completely unknown [44]. It is assumed that such a transition is connected with a change of the molecular conformation from a rod-like molecule in SmA, to a more bent molecule in the SmC phase. The stretching of the spacer is promoted by the decreasing temperature. Thus, on cooling the SmC$_c$ phase of **IV-*n*** the spacer stretches and a transition from SmC$_c$ to SmA$_c$ occurs. The enthalpy change associated with this transition is only 0.7 kJ mol^{-1}. The strong lateral interaction between the dipoles of adjacent mesogenic units might also play a role in this striking phenomenon.

3.5. *Comparison between series **I-n**, **II-n**, **III-n** and **IV-n***

In figure 10 the isotropization temperatures of all four series of compounds are compared. This figure clearly shows that the compounds of the series with a central aromatic part (**I-*n***) have the highest clearing temperatures. Non-symmetrical introduction of methyl substituents on the central pentyl spacer in the **III-*n*** series results in a decrease in isotropization temperatures as compared with the unsubstituted **II-*n*** series. Introduction of the substituents at the central carbon atom (series **IV-*n***), on the other hand, results in an increase in the isotropization temperatures, especially for the longer members of the series.

Comparison of the melting points of all four series (tables 1–4) shows that the influence of both symmetrical and non-symmetrical substitution is pronounced. The introduction of these substituents causes the melting points to drop by as much as 40°C as compared with those of the **II-*n*** series.

The **I-*n*** series differs in a number of ways from the

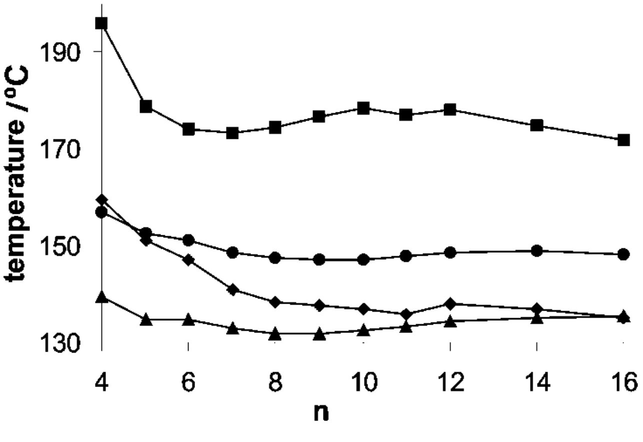

Figure 10. Dependence of the isotropization temperatures of the compounds of series **I-*n*** (—■—), **II-*n*** (—◆—), **III-*n*** (—▲—) and **IV-*n*** (—●—) on the number of carbon atoms n in the terminal chains.

other three series. The melting points, isotropization temperatures and phase behaviour are significantly different. The main reason for this different behaviour is probably related to the fact that the molecules of the **I-*n*** series can be regarded as liquid crystals with one mesogenic unit and two alkyl tails. As a result monolayer behaviour ($n=7$–16) is found, and because the mesogenic units have a bent shape they form banana-phases. The series with the flexible alkyl spacers (**II-*n***, **III-*n*** and **IV-*n***) can be regarded as liquid crystal dimers with significantly different mesomorphic properties.

The layer spacings of the **III-*n*** and **IV-*n*** series are shown in figure 11. The transition from the intercalated SmA_c to the intercalated SmC_c phase, as deduced from polarized light microscopy, is also clear from the deviation of a linear decrease of the layer spacing with decreasing *n*. The slightly larger layer spacings for the symmetrical **IV-*n*** compounds was anticipated. Thus the bulky dimethyl substituents give rise to steric hindrance which forces the molecules in the symmetrical **IV-*n*** series to adopt an irregular structure. For the non-symmetrical **III-*n*** series the molecules can be positioned in an alternating manner in which the steric hindrance is reduced.

The short homologues of all the series with flexible spacers (**II-*n***, **III-*n*** and **IV-*n***) exhibit the intercalated SmC_c phase, probably because of their relatively short terminal alkyl chains and the odd-numbered spacer. Intercalation for the longer homologues of series **III-*n*** and **IV-*n*** is caused by the substituents, which suppress the B_1 phase found in **II-*n***. In a B_1 phase there is local microphase separation in which the central aromatic parts, including the spacers of a number of molecules, are located in columns surrounded by the alkyl tails. By the introduction of dimethyl substituents, the spacer-spacer interaction in the B_1 phase becomes unfavourable. This unfavourable spacer-spacer interaction is reduced in the SmA_c phase. The fact that intercalated structures are found for all dimeric compounds (series **II-*n***, **III-*n*** and **IV-*n***) is probably caused by the possibility of the dipoles of the mesogenic groups to align antiparallel in the intercalated structures. With long terminal groups the interaction between the antiparallel dipoles of the mesogenic groups will be relatively weak. With decreasing terminal chain lengths these interactions will become stronger, which could result in the transition to the SmC_c phase. Because the layer thickness of the **IV-*n*** compounds is larger than for the **III-*n*** series, it is possible that this is the reason why the transition to SmC_c occurs for a shorter terminal tail in the **IV-*n*** series.

4. Conclusions

All 44 salicylaldimine-based compounds that have been synthesized exhibit liquid crystalline mesophases. The nature of the central part and length of the terminal alkyl chains has a remarkable influence on the mesomorphic properties. As in most banana-shaped liquid crystals, a phenyl or biphenyl central part promotes the formation of B-phases. For the **I-*n*** series three different B-phases were observed, and these show the phase sequence B_6–B_1–B_2 on increasing the terminal chain length. Replacement of the phenyl spacer (**I-*n***) with a pentyl spacer (**II-*n***) results in the partial disappearance of B-phases and formation of the intercalated SmC_c phase for the shorter homologues. The longer homologues ($n=8$–16) of the **II-*n*** series exhibit the two-dimensional B_1 phase.

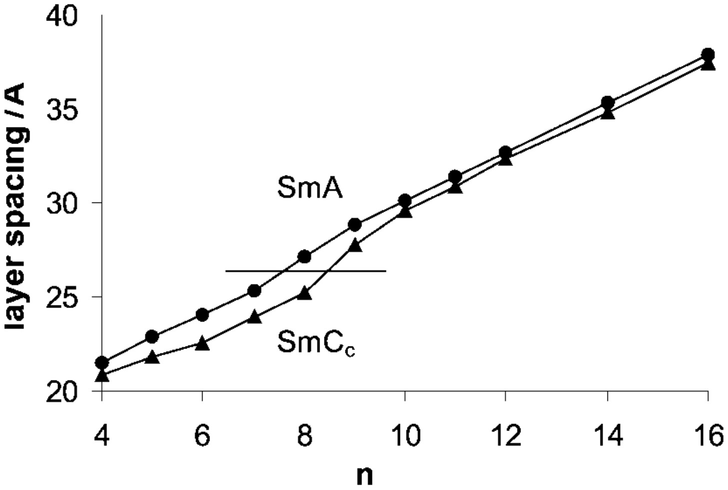

Figure 11. Layer spacings for the compounds of series **III-*n*** (—▲—) and **IV-*n*** (—●—) as a function of the number of carbon atoms ***n*** in the terminal chains.

The introduction of two methyl substituents to the central pentyl spacer (series **III-*n*** and **IV-*n***) dramatically depresses the melting temperatures, and also the formation of B-phases is suppressed, probably because of steric hindrance. Both substituted series exhibit the intercalated SmA_c phase for the longest homologues in spite of their odd-numbered spacers, whereas the short homologues exhibit the intercalated SmC_c phase. Thus the random mixing of the central part and terminal chains occurs for both phases. The occurrence of the unusual phase sequence $SmC_c \rightarrow SmA_c$ for **IV-4** on decreasing the temperature might be related to the stretching of the spacer which is promoted by decreasing temperature.

Although some dimeric compounds with an odd number of flexible units between the two mesogenic parts exhibit switchable B-phases, these phases are not so common as in compounds with a central phenyl or biphenyl segment. In the series described in this paper, replacement of the central phenyl group with a pentyl or substituted pentyl group results in the disappearance of the switchable B_2 phase.

The authors would like to thank Mr A. van Veldhuizen for NMR measurements and Mr E. van der Klift for elemental analysis. This work was financially supported by the Dutch Technology Foundation (STW). The research of Dr Z. Karczmarzyk has been made possible by a fellowship of the Netherlands Ministry of Agriculture, Nature Management and Fisheries.

References

[1] NIORI, T., SEKINE, F., WATANABE, J., FURUKAWA, T., and TAKEZOE, H., 1996, *J. mater. Chem.*, **6,** 1231.

[2] PELZL, G., DIELE, S., and WEISSFLOG, W., 1999, *Adv. Mater.*, **11,** 707.

[3] SALFETNIKOVA, J., SCHMALFUSS, H., NADASI, H., WEISSFLOG, W., and KRESSE, H., 2000, *Liq. Cryst.*, **27,** 1663.

[4] WATANABE, J., NIORI, T., SEKINE, T., and TAKEZOE, H., 1998, *Jpn. J. appl. Phys.*, **37,** L139.

[5] SHEN, D., PEGENAU, A., DIELE, S., WIRTH, I., and TSCHIERSKE, C., 2000, *J. Am. chem. Soc.*, **122,** 1593.

[6] DIELE, S., GRANDE, S., KRUTH, H., LISCKA, C., PELZL, G., WEISSFLOG, W., and WIRTH, I., 1998, *Ferroelectrics*, **212,** 169.

[7] PELZL, G., DIELE, S., JAKLI, A., LISCKA, C., WIRTH, I., and WEISSFLOG, W., 1999, *Liq. Cryst.*, **26,** 135.

[8] BEDEL, J. P., ROUILLON, J. C., MARCEROU, J. P., LAGUERRE, M., NGUYEN, H. T., and ACHARD, M. F., 2001, *Liq. Cryst.*, **28,** 1285.

[9] ROUILLON, J. C., MARCEROU, J. P., LAGUERRE, M., NGUYEN, H. T., and ACHARD, M. F., 2001, *J. mater. Chem.*, **11,** 2946.

[10] BEDEL, J. P., ROUILLON, J. C., MARCEROU, J. P., LAGUERRE, M., ACHARD, M. F., and NGUYEN, H. T., 2000, *Liq. Cryst.*, **27,** 103.

[11] HEPPKE, G., PARGHI, D. D., and SAWADE, H., 2000, *Liq. Cryst.*, **27,** 313.

[12] WEISSFLOG, W., WIRTH, I., DIELE, S., PELZL, G., SCHMALFUSS, H., SCHOSS, T., and WURFLINGER, A., 2001, *Liq. Cryst.*, **28,** 1603.

[13] PRASAD, V., 2001, *Liq. Cryst.*, **28,** 1115.

[14] RAUCH, S., BAULT, P., SAWADE, H., HEPPKE, G., NAIR, G. G., and JAKLI, A., 2002, *Phys. Rev. E*, **66,** 021706.

[15] SHEN, D., DIELE, S., WIRTH, I., and TSCHIERSKE, C., 1998, *Chem. Commun.*, 2573.

[16] WATANABE, J., IZUMI, T., NIORI, T., ZENNYOJI, M., TAKANISHI, Y., and TAKEZOE, H., 2000, *Mol. Cryst. liq. Cryst.*, **346,** 77.

[17] WATANABE, J., NIORI, T., CHOI, S.-W., TAKANISHI, Y., and TAKEZOE, H., 1998, *Jpn. J. appl. Phys.*, **37,** L401.

[18] CHOI, S.-W., ZENNYOJI, M., TAKANISHI, Y., TAKEZOE, H., NIORI, T., and WATANABE, J., 1999, *Mol. Cryst. liq. Cryst.*, **328,** 185.

[19] PRASAD, V., SHANKAR RAO, D. S., and KRISHNA PRASAD, S., 2001, *Liq. Cryst.*, **28,** 761.

[20] PRASAD, V., SHANKAR RAO, D. S., and KRISHNA PRASAD, S., 2000, *Liq. Cryst.*, **27,** 585.

[21] PRASAD, V., LEE, K.-H., PARK, Y. S., LEE, J.-W., OH, D.-K., HAN, D. Y., and JIN, J.-I., 2002, *Liq. Cryst.*, **29,** 1113.

[22] POCIECHA, D., KARDAS, D., GORECKA, E., SZYDLOWSKA, J., MIECZKOWSKI, J., and GUILLON, D., 2003, *J. mater. Chem.*, **13,** 34.

[23] AMARANATHA REDDY, R., and SADASHIVA, B. K., 2002, *J. mater. Chem.*, **12,** 2627.

[24] PELZL, G., EREMIN, A., DIELE, S., KRESSE, H., and WEISSFLOG, W., 2002, *J. mater. Chem.*, **12,** 2591.

[25] PELZL, G., DIELE, S., GRANDE, S., JAKLI, A., LISCHKA, C., KRESSE, H., SCHMALFUSS, H., WIRTH, I., and WEISSFLOG, W., 1999, *Liq. Cryst.*, **26,** 401.

[26] FODOR-CSORBA, K., VAJDA, A., GALLI, G., JAKLI, A., DEMUS, D., HOLLY, S., and GACS-BAITZ, E., 2002, *Macromol. Chem. Phys.*, **203,** 1556.

[27] KAŠPAR, M., HAMPLOVÁ, V., NOVOTNÁ, V., GLOGAROVÁ, M., and VANEK, P., 2002, *J. mater. Chem.*, **12,** 2221.

[28] WEISSFLOG, W., KOVALENKO, L., WIRTH, I., DIELE, S., PELZL, G., SCHMALFUSS, H., and KRESSE, H., 2000, *Liq. Cryst.*, **27,** 677.

[29] WIRTH, I., DIELE, S., EREMIN, A., PELZL, G., GRANDE, S., KOVALENKO, L., PANCENKO, N., and WEISSFLOG, W., 2001, *J. mater. Chem.*, **11,** 1642.

[30] WEISSFLOG, W., NADASI, H., DUNEMANN, U., PELZL, G., DIELE, S., EREMIN, A., and KRESSE, H., 2001, *J. mater. Chem.*, **11,** 2748.

[31] DEHNE, H., POTTER, M., SOKOLOWSKI, S., WEISSFLOG, W., DIELE, S., PELZL, G., WIRTH, I., KRESSE, H., SCHMALFUSS, H., and GRANDE, S., 2001, *Liq. Cryst.*, **28,** 1269.

[32] SHUBASHREE, S., SADASHIVA, B. K., and DHARA, S., 2002, *Liq. Cryst.*, **29,** 789.

[33] WALBA, D. M., KORBLOVA, E., SHAO, R., and CLARK, N. A., 2001, *J. mater. Chem.*, **11,** 2743.

[34] YELAMAGGAD, C. V., HIREMATH, U. S., ANITHA NAGAMANI, S., SHANKAR RAO, D. S., and KRISHNA PRASAD, S., 2001, *J. mater. Chem.*, **11,** 1818.

[35] SHANKAR RAO, D. S., NAIR, G. G., KRISHNA PRASAD, S., ANITHA NAGAMANI, S., and YELAMAGGAD, C. V., 2001, *Liq. Cryst.*, **28,** 1239.

[36] YELAMAGGAD, C. V., ANITHA NAGAMANI, S.,

HIREMATH, U. S., SHANKAR RAO, D. S., and KRISHNA PRASAD, S., 2002, *Liq. Cryst.*, **29,** 1401.

[37] EILBRACHT, P., ACKER, M., and TOTZAUER, W., 1983, *Chem. Ber.*, **116,** 238.

[38] AMARANATHA REDDY, R., and SADASHIVA, B. K., 2002, *Liq. Cryst.*, **29,** 1365.

[39] AMARANATHA REDDY, R., and SADASHIVA, B. K., 2003, *Liq. Cryst.*, **30,** 273.

[40] SHREENIVASA MURTHY, H. N., and SADASHIVA, B. K., 2002, *Liq. Cryst.*, **29,** 1223.

[41] DATE, R. W., IMRIE, C. T., LUCKHURST, G. R., and SEDDON, J. M., 1992, *Liq. Cryst.*, **12,** 203.

[42] IMRIE, C. T., and HENDERSON, P. A., 2002, *Curr. Opin. colloid interface Sci.*, **7,** 298.

[43] BLATCH, A. E., and LUCKHURST, G. R., 2000, *Liq. Cryst.*, **27,** 775.

[44] WEISSFLOG, W., LISCHKA, C., DIELE, S., WIRTH, I., and PELZL, G., 2000, *Liq. Cryst.*, **27,** 43.

[45] WATANABE, J., KOMURA, H., and NIORI, T., 1993, *Liq. Cryst.*, **13,** 455.